Chapter 7

The distortion effect in the Coastal Cordillera

Through the distortion analysis applied to the observations in Chapter 5, it was observed that the data of the Coastal Cordillera region could be best explained by a 2-D superposition model (section 5.1; small regional skew parameters, and section 5.2; good tensor decomposition fit). Moreover, the channeling model is seen to be valid, too.
The regional strikes found by the search of the minimum 3-D induction strength range between -25°N and -40°N (fig.6.12), contradicting the tensor decomposition results (section (5.2). The reason is the strong current channeling effect, analogous to the observation made by the anisotropy model example (section 6.2): the regional strike is not recovered at the sites influenced by stronger current channeling (fig.6.9).
The strike angles of 25°N - 40°N (c.c.w.) are nearly 45° apart from the corresponding local azimuths. In the coordinate system of the local azimuth the TE-mode tensor elements Z_{xy}, Z_{xx} have very small amplitudes, in accordance with the channeling model hypothesis (i.e., small amplitudes of the electric field parallel to the elongated conductor). This leads to unstable ρ_a and phase curves for the corresponding components, which worsen with the addition of noise. Therefore, rotating the tensor by $\pm 45°$ from the local coordinate system, can yield the most stable result, since the 45° rotation angle implies a similar weight of all components, with emphasis on the small TE-mode elements (Z_{xx}, Z_{xy}).
Thus, if 5° is the local azimuth of the current channeling, -40° would lead to an equal weight of all the tensor elements. In our field data, most of the near coast sites show this 45° angle difference. An example can be seen for sites GLO and ENG, which have a local azimuth of 5° and -30°, respectively, while the minimum 3-D induction strengths for site GLO are found at strike angles of -25° to -40° [1] and 10° for site ENG (figs.7.1, 7.2, 7.16 and 7.17). We can observe that the ρ_a and phase curves of the impedance elements in the measured coordinate system (fig.7.4) are not as stable as the ones rotated by the minimum 3-D induction strength strike angle (+10°; -25° in fig.7.3). The latter shows clearly stable curves, where the measured data coincides with the statistical expected values (e(phs); appendix D), thus indicating that

[1] The -25° strike angle corresponds to the multiple-site channeling analysis for the site arrays schematized in table 5.1, while a single site analysis results in a -40° regional strike for site GLO.

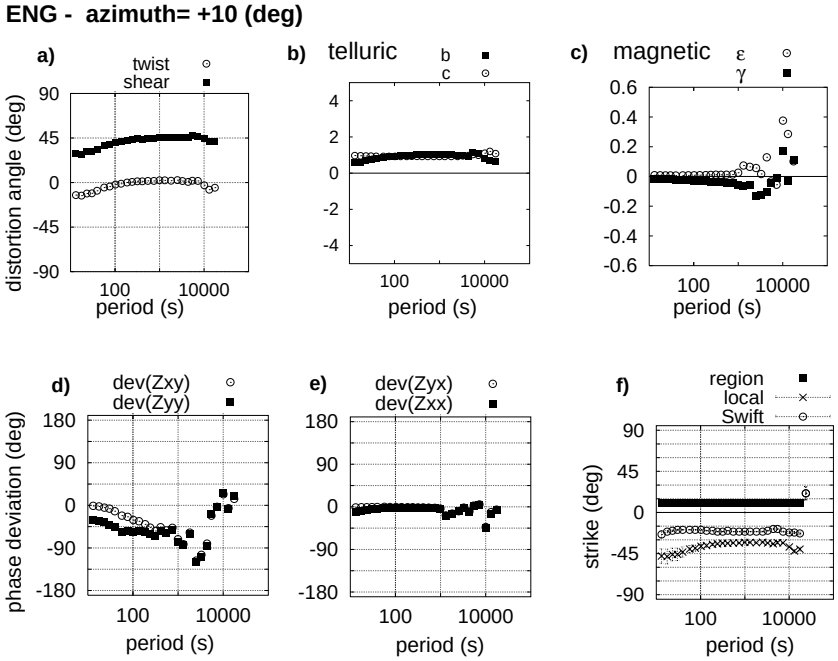

Figure 7.1: Distortion parameters of the channeling analysis for the field data: site ENG with a fixed strike angle of 10°, corresponding to the minimum 3-D induction strength. *a)* Twist and shear telluric angles, *b), c):* Telluric (b, c) and magnetic (γ, ε) distortion parameters. *d), e)* Phase deviations of the pairs of tensor elements. *f)* The regional strike (10°), the current channeling local azimuth (-30°) and the conventional Swift angle. By rotating the tensor to the local azimuth, TE-mode phases surpass 90° (fig.7.3).

the measured data are not biased in this coordinate system.

The confidence information that is recovered from the present analysis is the current channeling local azimuth regardless of the tensor coordinate system, provided that the channeling model is valid. The determination of the regional strike by the minimum 3-D induction strength fails for the case of extreme channeling effects or for very small electric field amplitudes.

What kind of conductivity structure causes the strong local current channeling observed in the near coast data? The induction arrows are a first hint of a non N-S strike structure, because if a pure ocean effect with a N-S coast line existed, the vectors would point E-W (fig.7.5a). The other observation is from the current channeling analysis. Small 3-D induction strengths were found only after rotating the tensor to the minimum value (-40 to -20°N; fig.6.13b), whereas at the 0° and -8°N fixed strikes a NNW-SSE trend of maximal 3-D induction strength is observed (figs.6.14 and 6.15). This NNW-SSE trend is in accordance with the local azimuths of the channeling model (i.e., the direction of local elongated conductors), determined for the MT data in any coordinate system having small channeling misfits (figs.6.13a, 6.14a) and 6.15a). Thus the hypothetical elongated conductors strike between -30°N and 5°N (fig.6.17), correlating with the orientation of the faults. This suggests that not only one but several elongated conductors of different azimuths can exist in the Coastal Cordillera. In this sense, a model of *sub-parallel conductivity structures* is met, since the elongated conductors are oriented near to the N-S direction, i.e., sub-parallel to the regional strike assumed to be given by the ocean structure (the coast line).

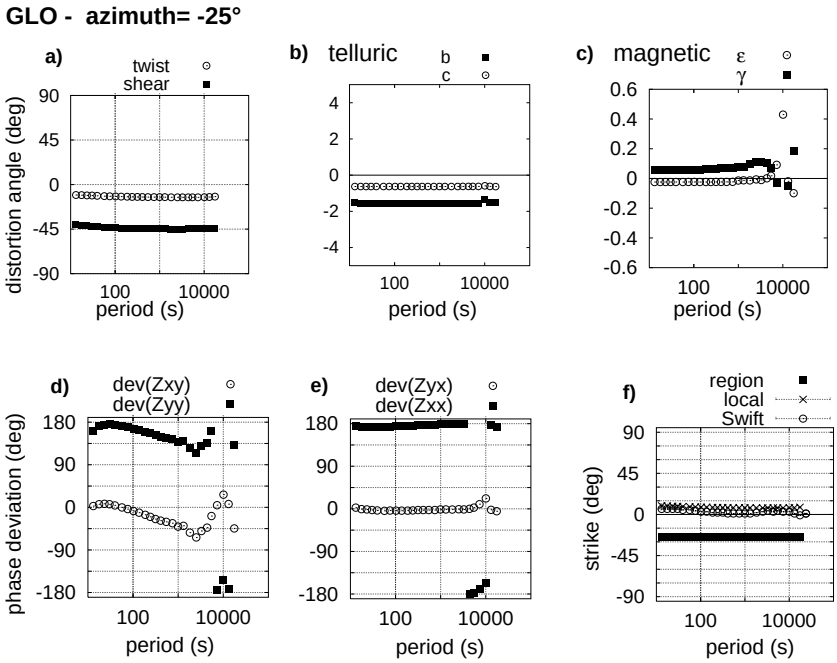

Figure 7.2: Distortion parameters of the channeling analysis for the field data: site GLO with a fixed strike angle of -25°, corresponding to the minimum 3-d induction strength. Explanation of the plots as in fig.7.1. The current channeling azimuth (rotational invariant) is 5°. By rotating the tensor to this local azimuth, TE-mode phases surpass 90° (fig.7.3). The equal (±180°) phase deviations between each tensor elements column (dev(Z_{xy}, Z_{yy}) dev(Z_{yx}, Z_{xx})) confirm the channeling model hypothesis.

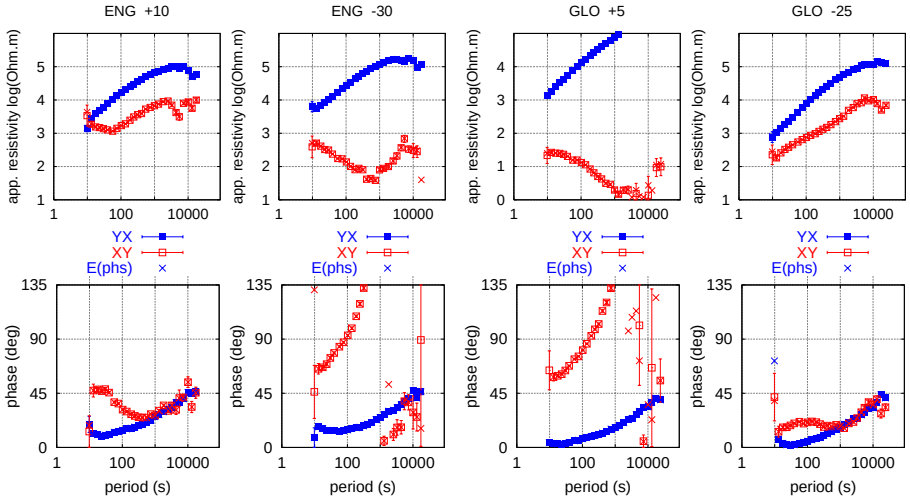

Figure 7.3: ρ_a and phase data of sites ENG and GLO. *ENG+10, GLO-25*: Tensor rotated to the coordinate system of the minimum 3-D induction strength. *ENG-30, GLO+5:* Tensor rotated to the channeling local azimuth (-30°N, 5°N). XY=TE-mode, E(phs)=expected value.

Based on the analysis mentioned above regarding the NNW-SSE orientation of the elongated conductors, the following section demonstrates with a simplified 3-D model for the region the distortion source characteristics that are necessary to obtain the anomalous TE-mode phases observed in the data. The 3-D modeling thus allows an interpretation of the conductivity structures required by the data.

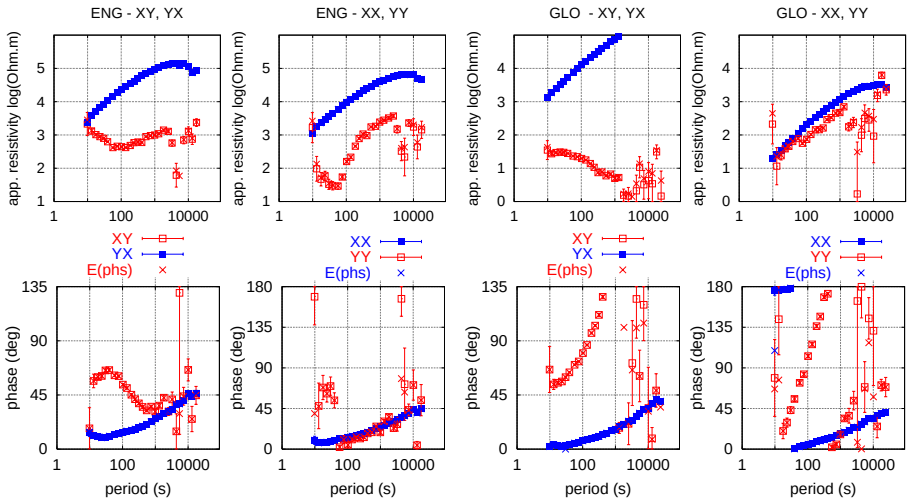

Figure 7.4: ρ_a and phase data of sites ENG and GLO in the measured coordinate system (NS). *ENG:* Left and right plots correspond to the off-diagonal (XY, YX) and diagonal (XX, YY) tensor elements. *GLO:* Idem for site GLO. E(phs)=expected value.

7.1 A qualitative 3-D model for the Coastal Cordillera

To investigate qualitatively the conductivity structure causing the distortion effects observed in the Coast data, a simple 3-D model study was performed with the forward code of Mackie & Booker (1999). In this (fig.7.5), the 2-D regional structure is a conductive ocean with resistivity values of 0.5-1 Ωm extending from the surface to 6-7 km of depth, followed by a resistive space (1000 Ωm) below. The local structure is a shallow elongated conductor (SEC) of 1 Ωm, rotated by 45° horizontally with respect to the regional strike (i.e., the angle θ of the channeling model; fig.6.3) and extends from 1 to 9 km of depths. It is embedded in a resistive space of 500-1000 Ωm. The deepest part of the model is low in resistivity (20 Ωm), thus simulating the average resistivity values associated with the upper mantle. This low resistive bottom layer is set deeper (300 km) beneath the ocean as in the 2-D model of the Pica profile developed by Echternacht [1998], in order to achieve a larger conductance[2] value beneath the continent. The 1000 Ωm block beneath the ocean increases the conductivity contrast between the oceanic and the continental lithospheres. Thereby the crustal current flow induced by the conductive ocean strengths, as was mentioned in the anisotropy model example (section 6.2).

The real parts of the induction arrows of the model response are shown for the period 100 s (fig.7.5b). Remarkably, they deviate from the x-axis (W-E) direction as would in a pure 2-D ocean structure, thus indicating the significant magnetic effects produced by SEC at this period. The induction arrows then become more W-E oriented with period, due to the attenuation of the local magnetic effect with the penetration depth (section 1.2.3). The NNW-SSE direction of the induction arrows of the measured data (fig.7.5a) correlates with the respective model response in the region between the ocean and SEC, supporting the existence of elongated conductors oriented NNW-SSE in the study area.

[2]Conductance (S) is the integrated conductivity (σ) estimated within a certain depth range (dz): $S = \int \sigma \, dz$.

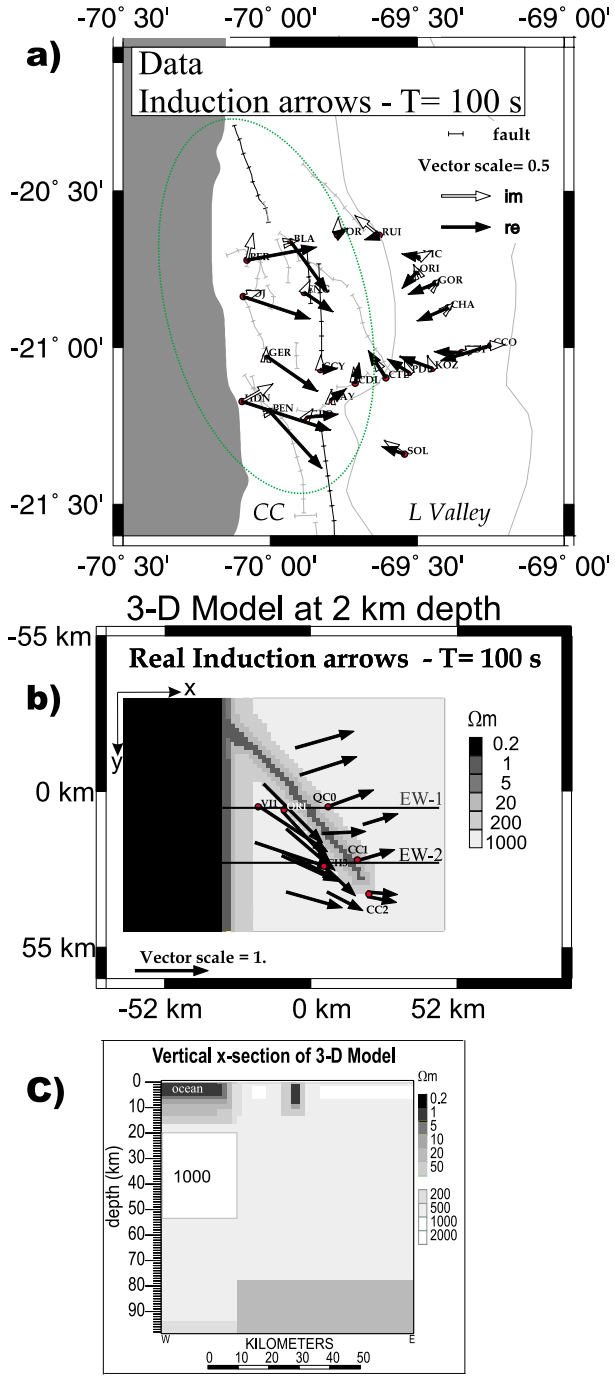

Figure 7.5:
3-D model to investigate the current channeling effect in the Coastal Cordillera. *a)* Real induction arrows of the Coastal Cordillera data at period 100 s. *b)* Horizontal plan view scaled in kilometers for a model depth of 2 km, where an elongated conductor is embedded in a resistive space of $1000\,\Omega\ m$. The high conductivity zone to the left (black) conforms the 2-D (Y-strike) regional structure, simulating the electrical properties of an ocean. The real parts of the induction arrows for the 100 s period are shown. The two horizontal lines (E-W1,2) indicate the profiles used for the channeling analysis. *c)* Vertical section along the horizontal x-axis, scaled in kilometers from the surface down to a 95 km depth (100 km $\approx 1°$).

The current channeling analysis has been applied to the model response based on the galvanic assumption of frequency independent distortion parameters (section 6.1.8), as was done in the anisotropy model example (section 6.2). The regional strike is determined for single sites, where a 2% error proportional to the tensor element magnitude was added on the model (response) impedances. The period average parameters were analysed in the period band 50-8000 s.

The single site regional strikes are plotted as function of site location, separately for each profile (EW-1 and -2; figs. 7.6, 7.7). Also, the 3-D induction strength (section 6.1.8), the averaged local azimuth (section 6.1.9) and the channeling misfit (section 6.1.10) are shown

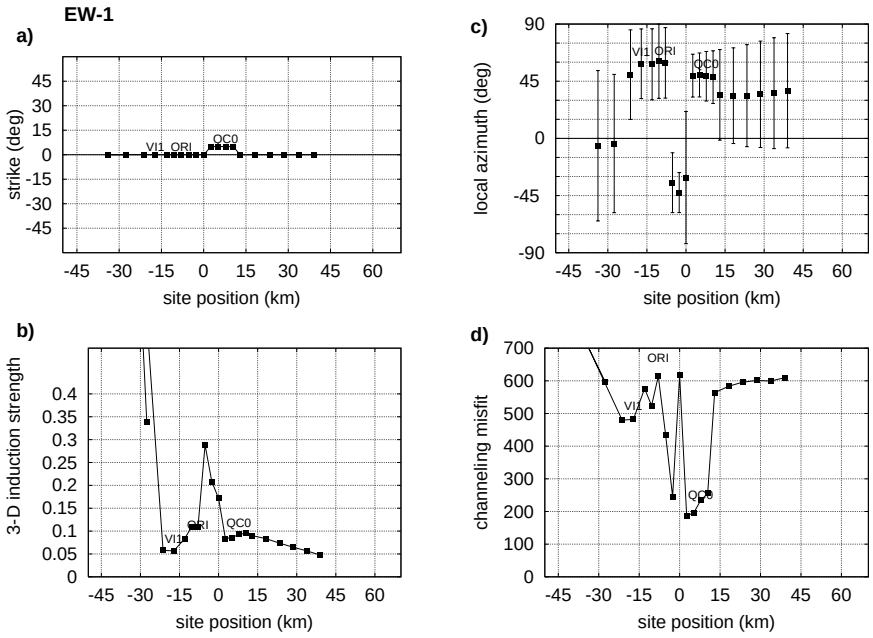

Figure 7.6: Distortion analysis (under the channeling assumption) for the EW-1 profile (in fig.7.5b). *a)* Frequency independent regional strike angles determined for single sites, found for the minimum 3-D induction strength (*b)*) estimated in the period band 50-8000 s. *c)* The averaged current channeling local azimuth for single sites with errors proportional to the channeling misfit (*d)*).

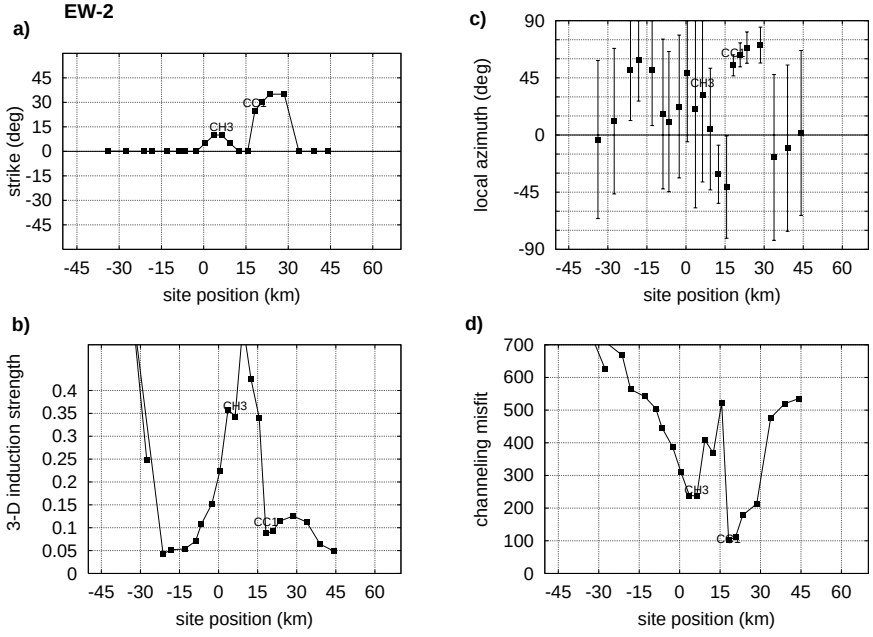

Figure 7.7: Parameter estimation of the channeling analysis for the EW-2 profile (in fig.7.5b). The explanation of each graphic is as in fig.7.6.

for the sites. The estimation of the single site local azimuth error and the channeling misfit normalized by the errors can be seen in the appendix (B.3.2, B.3.4).
The maximal 3-D induction strength occurs just above SEC (figs.7.6 and 7.7), where magnetic effects are strong. Moreover, the induction effect on the profile near the end of SEC (EW-2) is considerably greater than on EW-1 (i.e., greater 3-D induction strengths).
Strong channeling effects are seen at the sites located above the SEC borders, being even stronger on the side away from the ocean (sites QC0 and CC1 with smaller channeling misfit; figs. 7.6, 7.7). Also, the channeling effect is stronger at the profile crossing the near end of SEC (EW-2) than at the profile across the centre of SEC (EW-1). The minimum 3-D induction strength strike angles can not recover the real model strike (0°) in the regions affected by strong channeling effects, especially at the profile EW-2. The same can be observed by the anisotropy model (fig.6.9). In the study area, this observation is interpreted (in the second paragraph of section 7) as being due to data bias because of the small TE-mode electric field amplitudes.
The channeling misfit and the 3-D induction strength parameters indicate that the DC-currents concentrate at the edges of SEC differently (figs. 7.6, 7.7). The reasons are that the conductor is of limited extension and that the currents induced in the ocean have an influence as well.
In the regions where the channeling model is more appropriate (i.e., smaller channeling misfit at the borders of SEC), the local azimuth is around 45°, the direction of SEC (figs. 7.6, 7.7). Two sites are presented here to discuss the distortion characteristics of the analysis, where strong channeling effects are observed. The distortion parameters are the same as those shown in the anisotropy model example of section 6.2 (e.g., fig.6.8), corresponding to the superposition model (eq.6.11). The sites belong to different profiles and are located above the border of SEC, facing away to the ocean (sites QC0 and CC1; fig.7.5b). Figures 7.8 and 7.9 show the distortion parameters of site QC0 (EW-1 profile) and CC1 (EW-2), respectively, for a regional strike angle of 5° and 25° (c.w. with respect to the x-axis, i.e., W-E direction in geographical coordinates) corresponding to the minimum 3-D induction strength. The local azimuth determined by the channeling analysis, as well as the Swift angle[3] as a function of the period, are shown in these figures. Twist and shear deformation angles are relatively frequency independent, although they change smoothly in the period range 100-1000 s. The same is observed for the magnetic parameters. This reflects an inductive effect at the corresponding field penetration depths. The telluric parameters in contrast remain constant at all periods. Two more graphs show the phase deviations from the regional phases due to magnetic effect. They are either 0° or 180° at site QC0 (fig.7.8); thus almost no deviation is observed since the magnetic effect is small, while the phase deviations for site CC1 of the element pair Z_{yx}, Z_{xx} depart smoothly from 0° and 180° at period 1000 s, reflecting a non-negligible magnetic distortion effect at this polarisation mode. The maximal shear deformation angle (-45°) is better achieved at site CC1, which means that a stronger channeling effect occurs here than at QC0. The local azimuth at both sites lies near the real SEC direction (45-60° c.w. with respect to the x-axis).
By rotating the impedance tensor to the local azimuth of the current channeling the distortion

[3]The conventional Swift angle corresponds to the coordinate system where the diagonal tensor elements are minimal, which would indicate 2-D strike for a pure 2-D model.

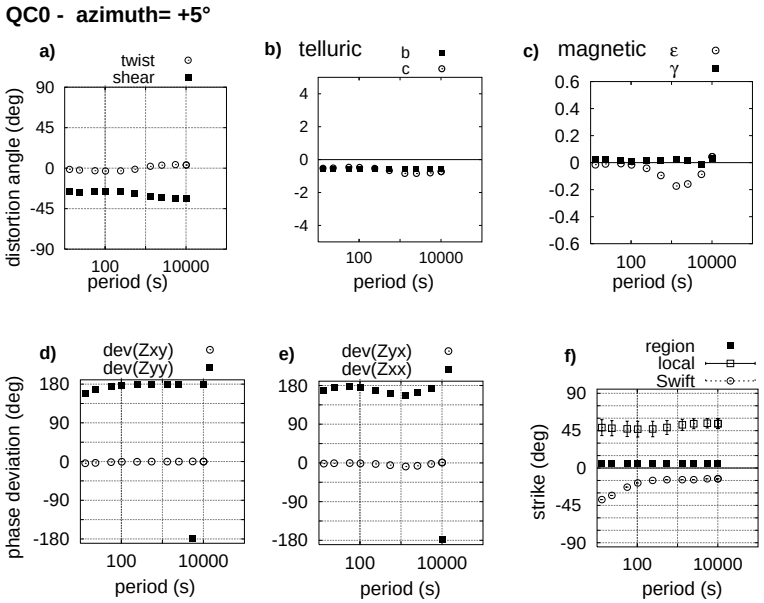

Figure 7.8: Illustration of the distortion parameters considered in the channeling analysis of the model response for site QC0, located on the boundary of SEC along the EW-1 profile (fig.7.5b). The tensor was rotated to the frequency independent angle (5°) of to the minimum 3-D induction strength at the period band 50-8000 s. *a)* Twist and shear telluric angles. *b)-c)* Telluric (b, c) and magnetic (γ, ε) distortion parameters, respectively. *d)-e)* Regional phase deviations for each pair of tensor elements ($dev(Z_{xy}) = \varphi$, $dev(Z_{yy}) = \alpha$, $dev(Z_{yx}) = \delta$, $dev(Z_{xx}) = \beta$) respectively. *f)* Regional strike (*region*), the *local* azimuth of the current channeling ($\sim 45°$ c.w., i.e., the SEC direction) and the conventional *Swift* angle.

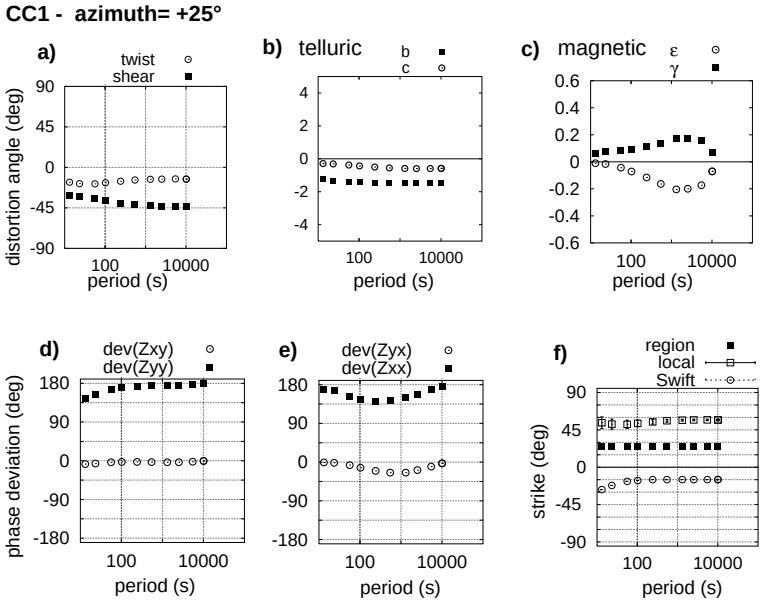

Figure 7.9: Distortion parameters considered in the channeling analysis of the model response for site CC1, located at the boundary of SEC along the EW-2 profile (fig.7.5b). Tensor rotated to the frequency independent angle (25°) of to the minimum 3-D induction strength at the period band 50-8000 s. Explanation of the graphs as in fig.7.8. Maximal telluric shear angles (45°) reflect strong current channeling, where magnetic distortions (γ, ε) are not negligible. The local azimuth is around 45° (c.w. with respect to x), i.e., the SEC direction.

characteristics expected for the *model of sub-parallel conductivity structures* (section 6.1.6) are observed. Especially at longer periods (figs. 7.10, 7.11), maximal and similar telluric deformation angles (*twist* $\approx$ *shear*) and the magnetic effect of the TE-polarisation mode is large ($\gamma \gg 0$), whereas that of the TM-polarisation mode vanishes ($\varepsilon \sim 0$). The property of equal phase deviations between the impedance pairs is not quite achieved, implying that induction effects are not negligible, which is also manifested in the frequency dependence of the distortion parameters (i.e., greater 3-D induction strengths). Therefore *the impedance tensor rotated to the local azimuth of the current channeling shows the maximal telluric deformation (twist and shear angles) as well as a large magnetic distortion manifested only in the TE-polarisation mode*[4]. And *this might lead the TE-mode regional impedance phases to shift to another quadrant, above* 90° (fig.7.12). The phases >90° are not only due to the magnetic effect. They can also be associated with a change of sign of the telluric deformation angles (twist and shear) at 1000 s, suggesting an extreme change in the direction of current flow. If the direction of current flow was changed by 180° by a specific conductor, assuming that the regional magnetic field remains unaltered (i.e., no magnetic distortion), the electric field component parallel to the flow would change its sign. Then the impedance phase of the corresponding polarisation mode would be shifted by ±180°, thus jumping from the I to the III quadrant (Egbert [1990]). However, it has been observed in the field data as well as in the model responses treated in this section and in 6.2 that large phase values beyond the I quadrant occur together with significant magnetic distortion effects.
At site QC0 the local azimuth has not been solved optimally, varying within a broad range (i.e., depends on the coordinate system), because the current channeling effect is not strong enough. But within this range, only at the rotation angle -15° does the TE-mode phases >90° occur. At site CC1 in contrast, the local azimuth (-30°) is more rotationally invariant since the current channeling is strong. Moreover, even at the 0° strike angle (the real regional strike) TE-mode phases >90° also occur. In the 0° coordinate system the TE-mode magnitude is too small (fig.7.14), resulting in unstable distortion parameters. Therefore the strike angle of the minimum 3-D induction strength (25°) for site CC1 corresponds to the more stable distortion parameters, where the small magnitude of the tensor elements have been up-weighted.

A similar situation is observed for a site located outside SEC, near to the southern boundary of it (fig.7.5b). The frequency independent strike angle found was 10° (c.w.), and the current channeling local azimuth found was around 60°-75° (c.w. with respect to the north), approximately parallel to the boundary of SEC. Here, the axis marks the main local conductivity contrast. These directions are more or less in agreement with the Swift angle, which ranges between 45° and 75° along the period band. The rotation of the impedance tensor to the current channeling local azimuth, where the telluric deformation as well as the magnetic effects of the TE-mode are maximal, results in an increase of the TE-mode impedance phases to another quadrant, surpassing 90°. Since a local azimuth of 70° is nearly perpendicular to the regional strike of the model, we illustrate the MT apparent resistivity and phases of the tensor rotated by -20° (fig.7.13) and refer to the tangential component as being sub-parallel to the regional strike. In this case, the TM-mode phase is the one strongly distorted by the magnetic distortion.

[4]The TE-mode refers here to the electric field tangential to the azimuth of the local conductor (SEC).

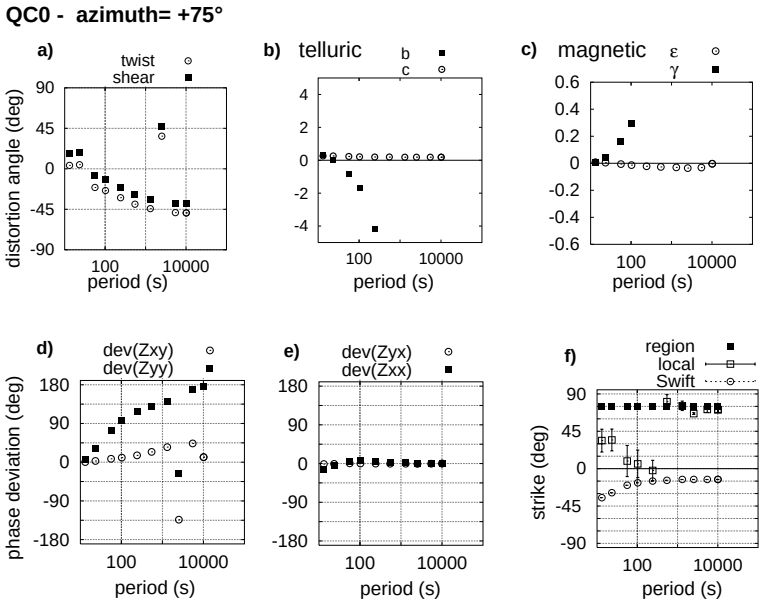

Figure 7.10: Distortion parameters of the model response for site QC0, located at the boundary of SEC along the EW-1 profile (fig.7.5b). The tensor was rotated to the local azimuth (75° c.w. with respect to the x-axis). The distortion characteristics of the *model of sub-parallel conductivity structures* are partly identified at long periods (see text for explanation). The graphs distribution as explained in fig.7.8. In some plots the distortion parameters b and γ are not shown because they surpass the usual values. In the local azimuth coordinate system, the TE-mode phases exceed 90° at long periods.

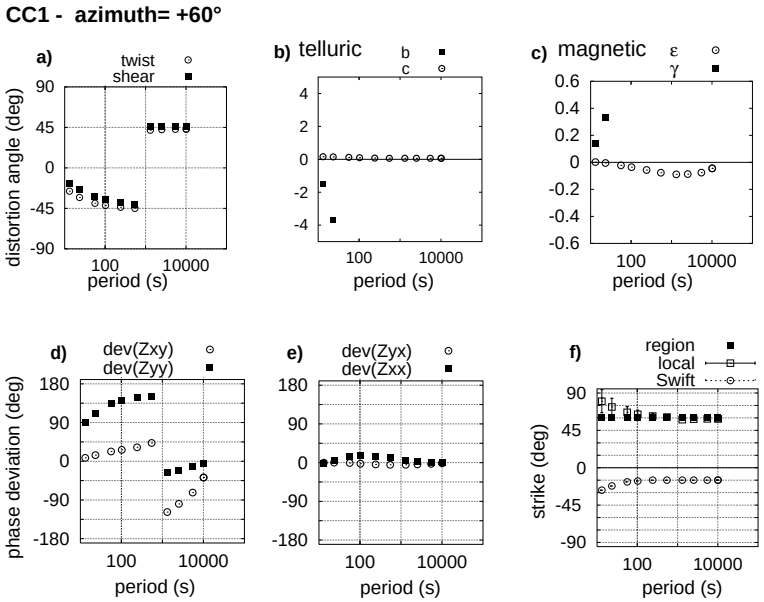

Figure 7.11: Distortion parameters of the model response for site CC1, located at the boundary of SEC along the EW-2 profile (fig.7.5b). The tensor was rotated to the local azimuth (60° c.w. with respect to the x-axis). The distortion characteristics of the *model of sub-parallel conductivity structures* are partly achieved at long periods (see text for explanation). The graphs distribution as explained in fig.7.8. In some plots the distortion parameters b and γ are not shown because they surpass the usual values. The TE-mode phases are close to 180° at long periods in the coordinate system of the local azimuth.

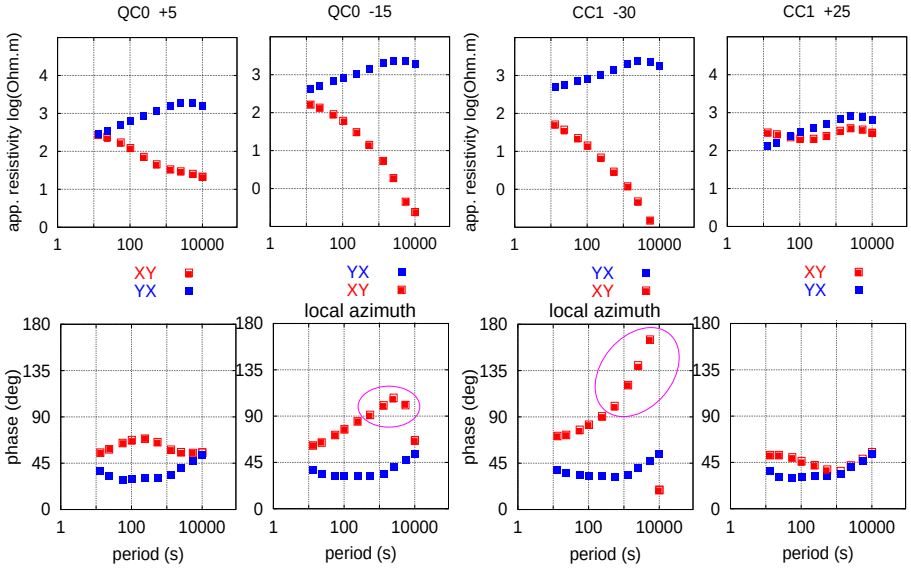

Figure 7.12: Apparent resistivities and phases of sites QC0 and CC1 of the model response (fig.7.5b) calculated at different coordinate systems (rotation is positive c.w. with respect to the north). *Left:* site QC0 +5 rotated by 5°, the angle of the minimum 3-D induction strength. QC0 -15 rotated by -15°, the angle of the local azimuth. *Right:* Site CC1 -30 rotated by -30°, the local azimuth, CC1 +25 rotated by 25°, the angle of the minimum 3-D induction strength.

The inductive coupling between the ocean and SEC produces such a current flow, inducing

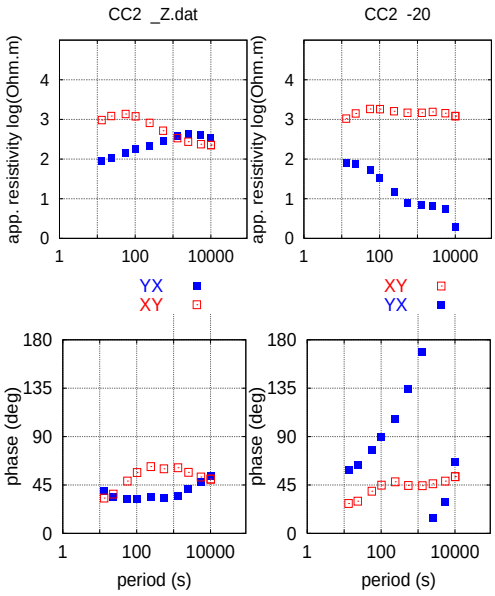

Figure 7.13: Apparent resistivities and phases of the 3-D model response for a site located outside the shallow elongated conductor (SEC), at the end of SEC (fig.7.5b). *Left:* The impedance tensor in the original coordinate system, i.e., the regional strike. *Right:* The impedance tensor rotated by 20° c.c.w. with respect to the north, which is the strike angle perpendicular to the SEC boundary orientation (i.e., the current channeling local azimuth).

anomalous magnetic fields as well, which leads to the anomalous phase behaviour (>90°) observed by one polarisation mode. This has been verified by comparing the responses of the 3-D model with the ocean subtracted, where no phases >90° occur (fig.7.14). The current channeling for the model without the ocean is also strong at the borders of SEC, as well as the induction effect above of it (fig.7.15). The magnetic distortion however is smaller with the ocean subtracted: the maximal 3-D induction strengths are concentrated narrowly above

SEC, whereas in the original 3-D model they expand in the direction of the ocean (fig.7.7), reflecting the inductive coupling between the ocean and SEC.

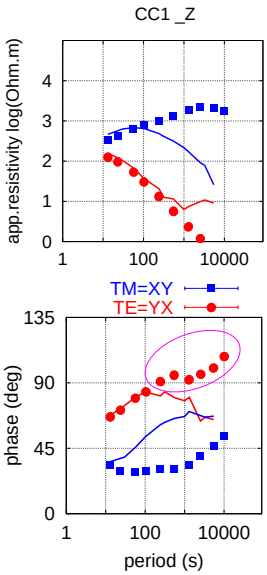

Figure 7.14: Apparent resistivities and phases of the 3-D model response (dots) and the response of the model without the ocean (lines) for site CC1, located above the border of the shallow elongated conductor on the EW-2 profile (fig.7.5b). The ellipsoid drawn on the bottom graph remarks the phases out of quadrant.

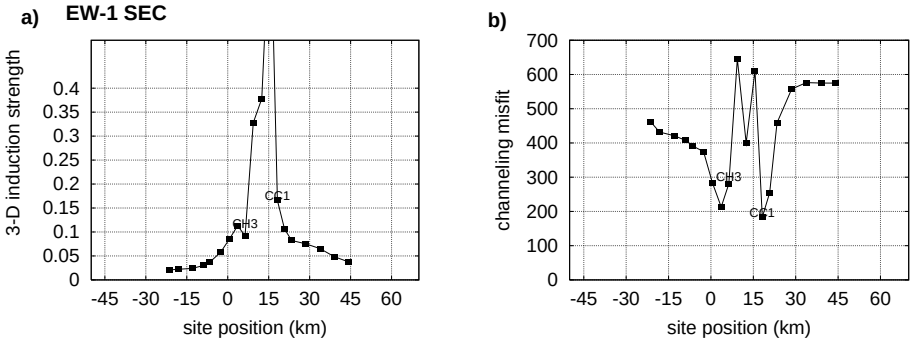

Figure 7.15: 3-D induction strength (*a)*) and channeling misfit (*b)*) for the profile EW-1 of the 3-D model (fig.7.5b) with the ocean subtracted.

7.2 Model interpretation

The similarities observed between the distortion parameters of the model response (figs. 7.10, 7.11) and that of the measured data (figs. 7.16, 7.17) permit us to assume that the Coastal Cordillera region has a similar conductivity structure as the 3-D model introduced here (fig.7.5).

Considering that the model responses also show TE-mode phases >90 in the coordinate system of the current channeling (fig.7.12), as can be observed in the measured data (fig.7.3), together with the estimated channeling local azimuths (red labels; fig.6.17), a model of horizontally elongated conductors following the Atacama fault system represent the region well. Since the local magnetic effects are not negligible (bottom plots; figs.6.13, 6.14 and 6.15), the induction arrows reflect the inductive coupling exerted between the ocean and the elongated

vertical dike(s) (fig.7.5a). The depth(s) of the dike(s) can be inferred from the behaviour of the induction arrows with changing period, provided that the background resistivity has already been determined.

The qualitative 3-D model study gives insight on the conductivity structure beneath the Coastal Cordillera as well as on the distortion source. The elongated conductor(s) of crustal depths oriented NNW-SSE together with the ocean effect is the reason for the distortion of the TE-polarisation mode data. In addition, the conductance values (integrated vertical conductivity) from the ocean lithosphere must be lower than that from the continent to strength the current channeling affected by a severe change of the direction of current flow at a certain penetration depth.
Under the idea of the "model of sub-parallel conductivity structures" introduced in section 6.1.6, i.e., elongated conductors as the local distorters coupled with the 2-D ocean effect −the structures oriented sub-parallel with each other−, we speak of the "2-D distortion effect" in the Coastal Cordillera, where the TE-polarization mode (coast parallel electric field) is distorted mainly by the current channeling.

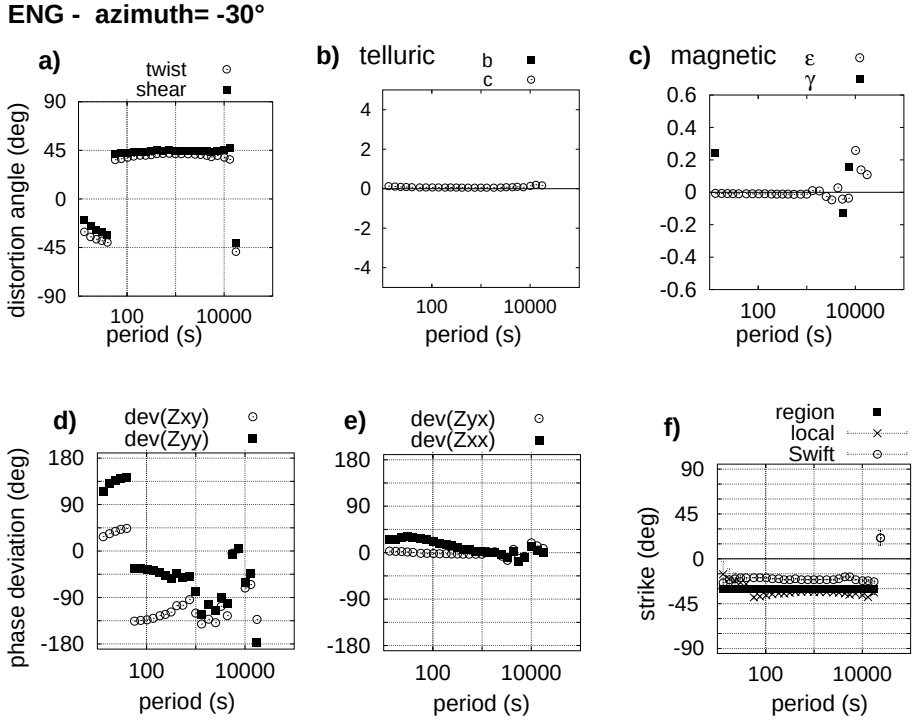

Figure 7.16: Distortion parameters of the channeling analysis for the measured data: site ENG rotated by -30°N, the channeling local azimuth (rotational invariant at longer periods). Explanation of the plots as in fig.7.1. By rotating the tensor to the local azimuth, TE-mode phases surpass 90° (fig.7.3).

7.3 The 2-D approach in the Coastal Cordillera

In order to investigate the ocean effect as well as to obtain the background (regional) conductivity values for further 3-D modeling, the 2-D regional approach will be applied to the

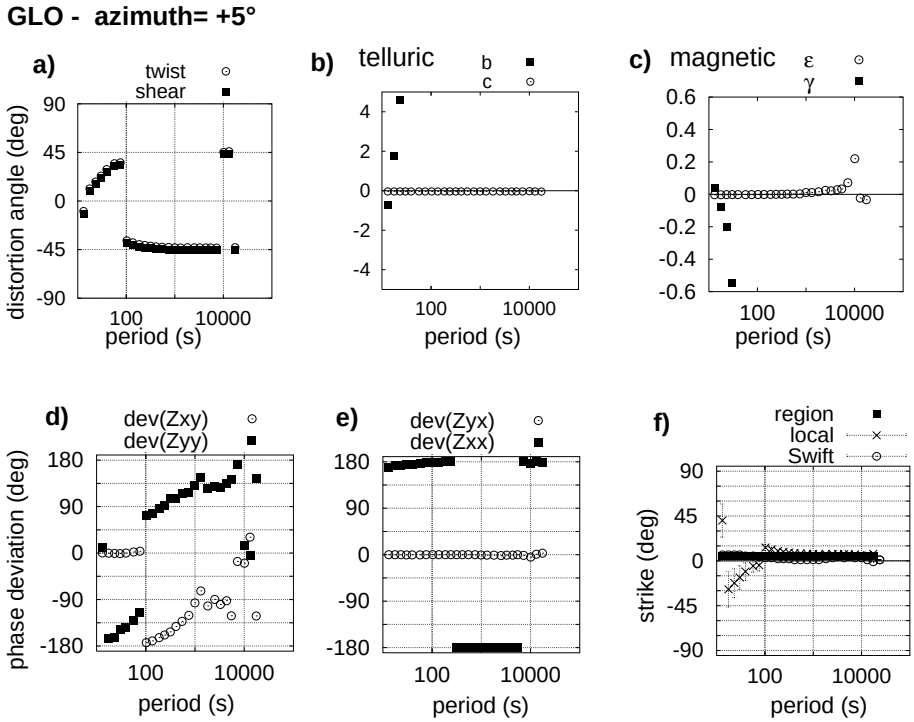

Figure 7.17: Distortion parameters of the channeling analysis for the measured data: site GLO rotated by 5°N, the channeling local azimuth (rotational invariant). Explanation of the plots as in fig.7.1. By rotating the tensor to the local azimuth, TE-mode phases surpass 90° (fig.7.3).

MT data. A N-S strike direction will be considered, regarding the geological units and the direction of the coastline. This strike is partly in accordance with the telluric tensor decomposition result (section 5.2.1; fig.5.4).

It has been already demonstrated that telluric and magnetic distortions are contained in the data of the Coastal Cordillera and affect the TE-mode (XY) impedance phases, resulting in values >90°.

The MT data can be approached by a 2-D tensor with the eigenvalues estimation formulated by Eggers [1982] (Section 1.2.2). Since this rotationally invariant procedure would best recover the 2-D tensor if galvanic effects are weak (Groom and Bailey [1991]), we are aware that this estimation is only an approximation of the actual removal of local effects.

Nevertheless, the correction of distortion by the eigenvalues estimation is supported by the 3-D model response for the sites shown in fig.7.18. The eigenvalues for the model with the included distorter (i.e., the elongated conductor; fig.7.5b) approximate the responses of a 2-D ocean model alone (in lines; fig.7.18). Only the static telluric distortion of the TE-mode has not been removed, which can be seen in the shifted ρ_a curves.

The eigenvalues of the measured impedance tensor are quite similar among sites (fig.7.19). Moreover, the eigenvalues give similar corrected TE-mode impedance phases as those estimated from the telluric and magnetic tensor decomposition by Smith [1997] for an assumed N-S regional strike (Section 6.1.7). This similarity supports that magnetic effects at the TE-mode are removed and hence a 2-D approach is feasible at least for periods below 1000 s. The discrepancies observed in the ρ_a curves are due to the undeterminacy of the static shift factors.

Due to the strong decay of the electric field amplitude with period in the TE-mode, data show large errors at periods >1000 s and they are subject to significant bias (statistical expected values e(phs); appendices C and D, departing from the measured value; fig.7.19). Thus the 2-D tensor recover is reliable only in the short period band (<1000 s) for the TE-mode.
The TM-mode phases are, in contrast, free of magnetic distortion, as was stated by the current channeling analysis for a model of sub-parallel conductivity structures (section 6.1.6), where the local currents distort only the TE-fields (approximately in N-S direction in the Coastal Cordillera). The TM- phase curves therefore remain unaltered after the correction procedure.

In **summary**, the eigenvalues allow a correction of the anomalous TE-mode (XY) phase behaviour, which is equivalent to a galvanic magnetic distortion removal for a N-S regional strike. The pseudo-section of the phase eigenvalues from the near coast data projected in a N-S profile shows more parallel contours than the original data (fig.7.20). The contours of the TM-mode phases are also close to parallel isolines, as expected for the N-S strike direction of a 2-D conductivity structure (i.e., of E-W lateral conductivity variations). The eigenvalues will be considered for the 2-D inversion modeling (Chapter 9).

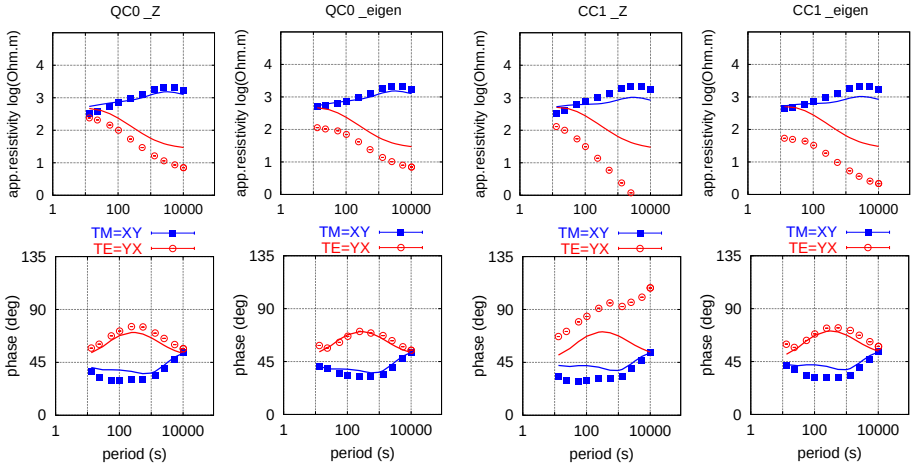

Figure 7.18: ρ_a and phase responses (*dots*) of site QC0 and CC1 of the 3-D model (fig.7.5b). The tensor is illustrated in the original coordinate system (*_Z*), and its eigenvalue (*_eigen*). The *lines* are the responses of the model without the elongated conductor, i.e., a 2-D ocean model.

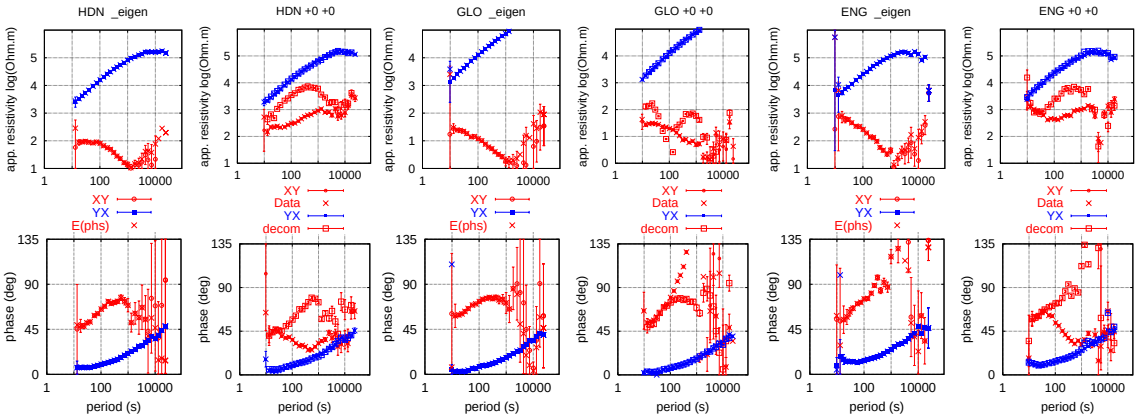

Figure 7.19: ρ_a and phase data of sites HDN, ENG and GLO. *_eigen:* Eigen values of the impedance tensor (rotational invariant). *+0 +0 :* Tensor corrected by the telluric and magnetic tensor decomposition treated in the N-S (=X) regional strike (open squares; *decom*) against the original data (XY,YX). E(phs)=expected value of the measured data.

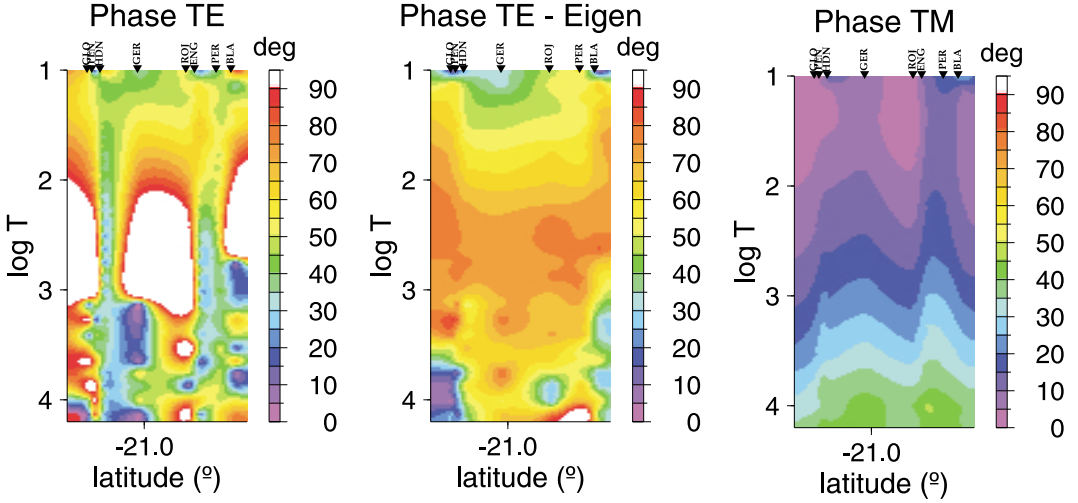

Figure 7.20: Phase pseudo-sections as function of logarithmic period (log T) of the near coast site data projected on N-S profiles. *Phase TE:* TE-mode phases (i.e., N-S electric field) of original data, *TE - Eigen:* Eigenvalues of the TE-mode phases, *Phase TM:* TM-mode phases of original data (strike = N-S).